Influence of High Level Features of HVS on Performance of FSIM

Petr DOSTÁL, Lukáš KRASULA, Miloš KLÍMA

Dept. of Radioelectronics, Czech Technical University in Prague, Technická 2, 166 27 Prague 6, Czech Republic

petr.dostal@fel.cvut.cz, krasuluk@fel.cvut.cz, klima@fel.cvut.cz

Abstract. *In this paper the influence of information about high level features of Human Visual System (HVS) on objective quality assessment is studied. This was done by extending the existing full-reference objective image quality metric – FSIM – where the different importance of certain areas of image is considered using Phase Congruency (PC) algorithm. Here, the estimation of Region of Interest (ROI) based on this algorithm is complemented by Fixation Density Maps (FDM) containing the information about high level features of HVS. Use of another low level features based algorithm (Phase Spectrum of Fourier Transform) was also considered and compared to the PC algorithm. The performance was evaluated qualitatively on images reconstructed according to ROI and quantitatively on images from LIVE database. The correlation between subjective and objective tests was calculated using Pearson's Correlation Coefficient and Spearman's Rank Order Coefficient. The statistical significance of the difference between correlation coefficients was assessed by Fisher r-to-z transformation. The performance of the metric was also compared to other state-of-the-art image quality metrics (SSIM, MS-SSIM, and FSIM).*

Keywords

Human visual system, image quality assessment, high level features, FSIM.

1. Introduction

The image and video quality assessment is very important issue in various fields of image and video processing because every processing algorithm affects the output quality and it is necessary to reliably evaluate its impact.

Basically, there are two ways how to assess the quality of images. The first way is the subjective quality testing, using the group of observers. During these tests, every subject evaluates the series of images, according to a procedure, such as Double-Stimulus Impairment Scale (DSIS) or Double-Stimulus Continuous Quality Scale (DSCQS). The most important procedures for subjective quality tests are described in ITU-R Recommendation BT.500-13 [1]. After the processing of results, the final values are Mean Opinion Scores (MOS) and standard deviations. That represents the quality perceived by the "average observer." This testing is really reliable but expensive, time-consuming, vulnerable to systematic errors etc. The other approach is based on utilization of objective image quality metrics. These are the algorithms able to automatically assess the quality of images. They could be divided to full-reference where the whole unprocessed image is necessary for evaluation, reduced-reference where only partial information (e.g. about edges) from the original image is needed and finally no-reference or blind image quality metrics which assess the quality with no further information than the image itself. The main advantages of objective metrics are that they are cheap, fast, and their results are unambiguous. The problem is that they are dependent on the content of images.

Most of the effort is so far done in the full-reference quality metrics area. The oldest ones are pixel-based criteria which come from the theory of signals. Mean Squared Error (MSE) and Peak Signal to Noise Ratio (PSNR) are the typical example of these metrics. The other important family of full-reference metrics is metrics based on the calculation of the loss of information during the process. The most important of these criteria is visual information fidelity (VIF) proposed by Sheikh [2]. Probably the most widely studied metrics are based on Human Visual System (HVS). The principle is to model human perception. The most popular HVS-based criteria are structural similarity index (SSIM) and multi scale SSIM (MS-SSIM) both proposed by Wang [3], [4]. The majority of these metrics however do not consider the fact that some areas in the image are of higher importance for observer than the other. One of the metrics which tries to include this kind of information is feature similarity index (FSIM) proposed by Zhang [5].

The areas containing the most visual information are called Region of Interest (ROI). These regions are localized during the pre-attentive stage and further explored during the attentive stage [6]. There are two mechanisms influencing the visual attention [7].

Fig. 1. Image "Woman" from the LIVE database [11] and extracted low-level features – (a) original, (b) PC, (c) G, (d) PFT, (e) PC&PFT.

The bottom-up mechanism drives the attention, according to the content of the image, to the areas with e.g. contrast changes, edges etc.

The top-down mechanism is on the other hand influenced by the given task (e.g. traffic signs localization in the image) or the experience of the observer with the content of the image. The features extracted from the scene by these two mechanisms are either low level (LLF) – extracted by bottom-up mechanism – or high level (HLF) – extracted by top-down mechanism [7].

Naturally, it is very difficult to automatically estimate HLF from the scene. In this case, Fixation Density Maps (FDMs) obtained by the eye-tracking experiment are used [8]. FDMs show ROI obtained from both LLF and HLF.

In this paper, we investigate the influence of addition of the information about HLF in the quality metric on its performance compared to the subjective tests. It is the extension of our previous work, published in [9]. Here, the metric's performance is qualitatively tested in the context of multimedia imaging and thorough statistical analysis is applied to verify the significance of the results.

The paper is organized as follows: Section 2 describes the FSIM metric and its extensions done for the purpose of this paper, in Section 3 qualitative and quantitative results are presented and Section 4 concludes the paper. The illustrational scheme of High Level FSIM (HLFSIM) calculation could be found in Appendix.

2. Metric Extension

This section is dedicated to the description of FSIM, proposed modifications for LLF extraction, HLF information addition and HLFSIM calculation.

2.1 FSIM

The Feature Similarity Index is full-reference objective image quality metric proposed by Zhang [5]. Within FSIM, two main measures are employed.

The first one is Phase Congruency (PC) [10] which measures the significance of a local structure. It is based on the theory, that the features in image are perceived at points, where Fourier components are maximal in phase. It is defined as

$$PC(x) = \max_{\bar{\phi}(x)\in[0,2\pi]} \frac{\sum_n \left[A_n \cdot \cos(\phi_n(x) - \bar{\phi}(x))\right]}{\sum_n A_n} \quad (1)$$

where A_n is the amplitude of n-th Fourier component, $\Phi_n(x)$ denotes local phase of n-th Fourier component at position x and $\bar{\Phi}(x)$ means the amplitude weighted mean local phase angle of all the Fourier terms at position x.

In FSIM implementation, PC is calculated using bank of log-Gabor filters uniformly dividing the frequency plane. This method was proposed by Kovesi [11]. LLF map obtained by this calculation contains values from 0 to 1. An example of this map for image "Woman" (Fig. 1(a)) from LIVE database [12] is shown in Fig. 1(b).

The second measure used in FSIM is Gradient Magnitude (G). First, the gradient is calculated in horizontal and vertical direction by convolution of an image and Scharr operator [13]. Then G is calculated as

$$G = \sqrt{G_x^2 + G_y^2} \quad (2)$$

where G_x and G_y stand for gradient calculated in horizontal and vertical direction, respectively. Gradient Magnitude for "Woman" scene can be seen in Fig. 1(c).

Similarity between original and distorted image is calculated separately for both measures as

$$S_{Feature}(x) = \frac{2 \cdot Feature_1(x) \cdot Feature_2(x) + T_{Feature}}{Feature_1^2(x) + Feature_2^2(x) + T_{Feature}} \quad (3)$$

where $S_{\{.\}}$ denotes similarity map, *Feature* represents $PC(x)$ or $G(x)$ and indexes 1 and 2 indicate reference and distorted image, respectively. $T_{Feature}$ is small positive constant ensuring the fraction stability.

In the next stage, the information about ROI is used, to weight the similarity map according to the importance of

the area in the scene. The weighting map is the combination of PC maps from both original and distorted image:

$$PC_m(x) = \max[PC_1(x), PC_2(x)] \tag{4}$$

where $PC_m(x)$ stands for combined PC map and $PC_1(x)$ and $PC_2(x)$ represent PC maps from both scenes.

Finally, the FSIM index is calculated as

$$FSIM = \frac{\sum_{x\in\Omega} S_{PC}(x)\cdot S_G(x)\cdot PC_m(x)}{\sum_{x\in\Omega} PC_m(x)} \tag{5}$$

where Ω represents the whole image spatial domain.

2.2 FSIM$_C$

The above described procedure calculates with luminance component of the image only. Zhang [5] also defines the metric for colored input images.

First, the image is converted to YIQ color space [14]. Then the similarity $S_I(x)$ and $S_Q(x)$ for chrominance components I and Q is calculated according to (3).

Final index is then

$$FSIM_C = \frac{\sum_{x\in\Omega} S_{PC}(x)S_G(x)[S_I(x)S_Q(x)]^{\lambda} PC_m(x)}{\sum_{x\in\Omega} PC_m(x)} \tag{6}$$

where λ is a parameter influencing the importance of the chrominance components. This parameter was set to 0.03. The scheme of the whole procedure is the same as the one shown in Appendix, when $LLF_i = PC_i$ and $HLF = 1$. For more details refer to the relevant paper [5].

2.3 Modification of LLF Extraction

As mentioned before, the original FSIM index employs PC to extract LLF from the scene. In this paper, authors employed also another method for LLF extraction – Phase Spectrum of Fourier Transform (PFT) – and investigated if it can improve the metric performance.

Hou [15] proposed a method for localization of important areas in the scene based on spectral residual of an image. This is calculated from the log amplitude spectrum. However, Guo et al. [16] found out that the information about LLF is carried by the phase spectrum only. So they proposed the calculation of the LLF map:

$$PFT(x) = h_{\text{gauss}}(x) * [F^{-1}\{e^{i\cdot p(x)}\}]^2 \tag{7}$$

where $h_{\text{gauss}}(x)$ is a Gaussian kernel, * convolution operator, F^{-1} is an operator of inverse Fourier transform and i is the imaginary unit. PFT map is then normalized. An example is shown in Fig. 1(d).

Authors also combined these two methods:

$$PC\ \&\ PFT(x) = \max[PC(x), PFT(x)]. \tag{8}$$

LLF map obtained by this combination is in Fig. 1(e).

2.4 HLF Information Addition

Obtaining the information about HLF automatically is not an easy task because it requires modeling of complicated operations in human brain. Since this is not yet possible, all of the ROI estimators are so far based on LLF. That is why the use of Fixation Density Maps (FDMs) obtained by the eye-tracking experiment with human observers was necessary for including also the HLF information. FDM for Woman scene is depicted in Fig. 2(a).

(a) (b)

Fig. 2. Fixation Density Map and Importance Map for "Woman" scene.

To integrate it into the metric, the Importance map $I_{\text{map}}(x)$ is defined as

$$I_{\text{map}}(x) = LLF(x).\times HLF(x)\,. \tag{9}$$

Operator .× means point-by-point multiplication. $LLF(x)$ is a map obtained by

$$LLF(x) = \max[method_1(x), method_2(x)] \tag{10}$$

where $method_1(x)$ denotes the LLF map for original image obtained by one of the LLF extraction methods stated above or their combination. Index 2 labels the distorted image. Fig. 2(b) shows the Importance map for "Woman" scene.

2.5 HLFSIM Calculation

Similarity $S_{LLF}(x)$ between two LLF maps LLF_1 for original image and LLF_2 for distorted is obtained according to (3).

Finally, the HLFSIM index can be calculated similarly to FSIM:

$$HLFSIM = \frac{\sum_{x\in\Omega} S_{LLF}(x)\cdot S_G(x)\cdot I_{\text{map}}(x)}{\sum_{x\in\Omega} I_{\text{map}}(x)}. \tag{11}$$

Also the variant for colored images is

$$HLFSIM_C = \frac{\sum_{x\in\Omega} S_{LLF}(x)S_G(x)[S_I(x)S_Q(x)]^{\lambda} I_{\text{map}}(x)}{\sum_{x\in\Omega} I_{\text{map}}(x)}. \tag{12}$$

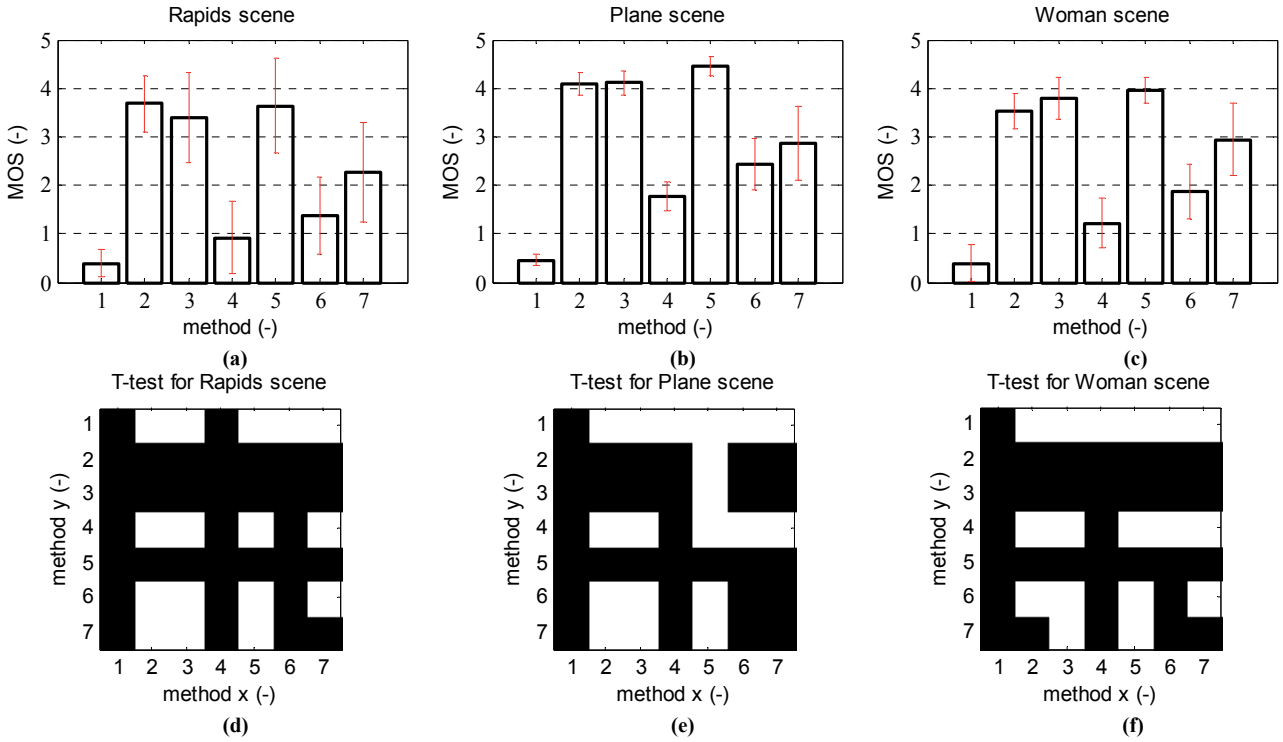

Fig. 3. The results of subjective tests and t-tests for images reconstructed according to ROI [17].

The graphical computation scheme of HLFSIM can be also found in Appendix.

3. Experimental Results

This section is dedicated to metric performance evaluation results. First, the metric was tested on images reconstructed according to ROI and then the quantitative analysis of performance on LIVE database [12] was conducted.

3.1 Performance of Common Metrics for Images Reconstructed According to ROI

In authors' previous work [17] a demosaicing technique using ROI for reconstruction was proposed. It is based on idea to reconstruct salient areas by interpolation technique with high quality performance and non-salient regions by some simple and fast method. Excessive subjective test were conducted to find out if the proposed method can outperform some of the common demosaicing techniques and therefore is applicable. MOS values and confidence intervals at significance level 0.05 from subjective results for three images from LIVE database [12] (Rapids, Plane and Woman) can be found in Fig. 3(a–c). Proposed methods (columns no. 6 and 7) were compared to following interpolation techniques: 1 – bilinear, 2 – Hirakawa's [18], 3 – Menon's [19], 4 – Alleyson's [20] and 5 – Chung's [21]. To verify if the quality difference between techniques is statistically significant, two sampled right tailed t-tests at significance level 0.05, similar to those done by De Simone [22], were performed. The results for aforementioned images are shown in Fig. 3(d–f). If the square between two methods is white, the method on the horizontal axis performs significantly better than the one on vertical axis. Otherwise the square is black. As can be seen, the method no. 7 outperforms Alleyson's algorithm (method no. 4). For more information about test conditions refer to the above mentioned work [17].

Quality assessment by objective criteria (Fig. 4(a–c)) was then performed using four state-of-the-art metrics (SSIM [3], MS-SSIM [4], FSIM [5] and $FSIM_C$ [5]). The results exhibit the contradiction between subjective and objective criteria (Alleyson's method in column 4 is evaluated to be better than the method in column 7) even for FSIM metric where the information about ROI is embedded. That leads to a conclusion that HLF information is also important for human quality perception and could be included in the quality metric.

3.2 Performance of HLFSIM for Images Reconstructed According to ROI

This part of the paper deals with the evaluation of performance of proposed metric on the images mentioned in previous paragraph. Results of the assessment done by HLFSIM and $HLFSIM_C$ in all three modifications (using PC, PFT and PC&PFT) are depicted in Fig. 4(d–f). It clearly shows the improvement in agreement with subjective tests.

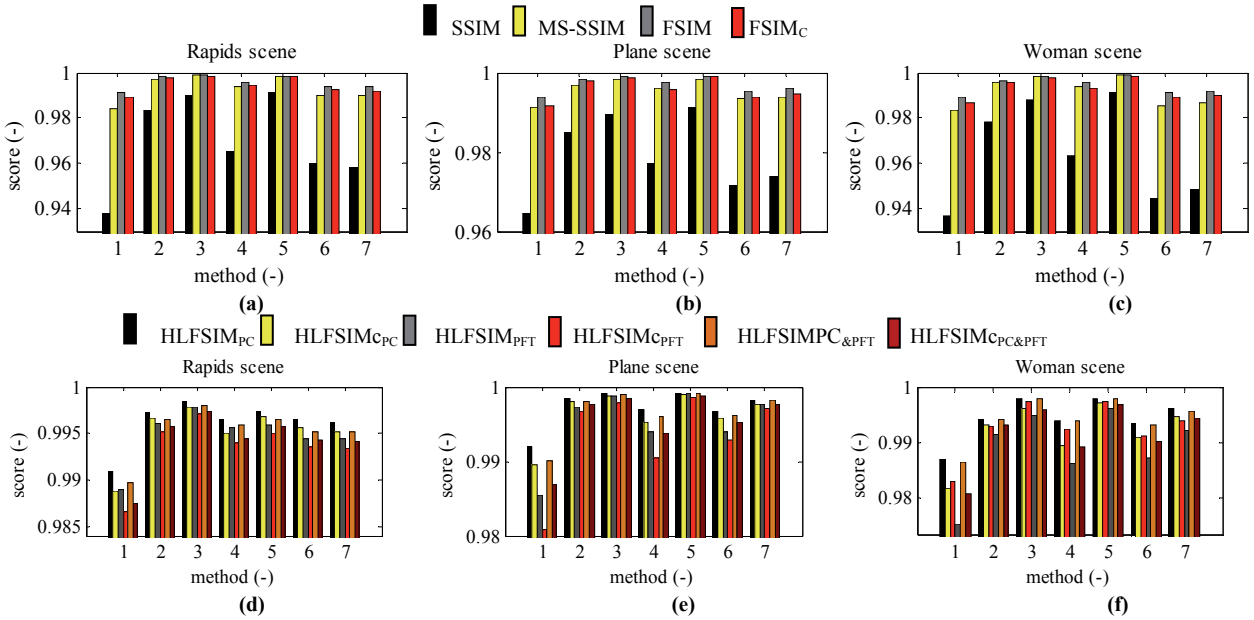

Fig. 4. The results of objective quality assessment for images reconstructed according to ROI [17].

Distortion	CC	SSIM	MS-SSIM	FSIM		$HLFSIM_{PC}$		$HLFSIM_{PFT}$		$HLFSIM_{PC\&PFT}$	
				lum	chrom	lum	chrom	lum	chrom	lum	chrom
JPEG	**PLCC (-)**	0.889	0.864	0.872	0.869	0.876	0.874	0.843	0.841	**0.879**	0.877
	SROCC (-)	0.930	0.951	**0.957**	**0.957**	0.955	0.954	0.949	0.948	0.954	0.955
JPEG2000	**PLCC (-)**	0.846	0.790	0.734	0.728	0.737	0.730	**0.743**	0.736	0.741	0.735
	SROCC (-)	0.900	0.911	0.913	0.913	**0.915**	0.914	0.914	0.913	**0.915**	0.914
White Noise	**PLCC (-)**	0.967	0.956	0.926	0.908	0.934	0.919	0.930	0.917	**0.937**	0.926
	SROCC (-)	0.968	0.975	0.972	0.965	0.981	0.976	0.981	0.978	**0.983**	0.981
Gaussian Blur	**PLCC (-)**	0.833	0.883	**0.909**	**0.909**	0.898	0.898	0.882	0.882	0.907	0.907
	SROCC (-)	0.882	0.947	**0.971**	**0.971**	0.969	0.969	0.959	0.959	0.966	0.966
Fast Fading	**PLCC (-)**	0.893	0.855	0.852	0.851	0.859	0.858	**0.889**	0.887	0.883	0.882
	SROCC (-)	0.938	0.953	0.951	0.950	0.950	0.947	**0.959**	0.956	0.954	0.952
All	**PLCC (-)**	0.717	0.731	0.774	0.780	0.788	**0.792**	0.779	0.781	0.785	0.791
	SROCC (-)	0.848	0.900	0.920	0.923	0.924	**0.925**	0.915	0.915	0.919	0.921

Tab. 1. Correlation between subjective and objective quality assessment results for LIVE database [12].

Distortion	$HLFSIM_{PC}$		$HLFSIM_{PFT}$		$HLFSIM_{PC\&PFT}$	
	lum	chrom	lum	lum	chrom	lum
JPEG	0.4286	0.4129	-	-	0.3745	0.3594
JPEG2000	0.4721	0.4801	0.4168	0.4286	0.4364	0.4364
White Noise	0.2912	0.2676	0.3936	0.3085	0.2207	0.1469
Gaussian Blur	-	-	-	-	-	-
Fast Fading	0.4052	0.4052	0.0778	0.0853	0.1230	0.1230
All	0.2389	0.2676	0.4013	0.4801	0.2912	0.2843

Tab. 2. Significance of difference tests – p-values.

3.3 Performance of HLFSIM for LIVE Database

Here, the quantitative evaluation of performance is described. It was done on images from LIVE database created by Sheikh [12]. It contains 29 reference images modified by different degrees of five types of distortions. These are compressions JPEG (233 images) and JPEG2000 (227 images), white noise (174 images), Gaussian blur (174 images) and simulation of fast fading Rayleigh channel (174 images). Database also provides the results of subjective tests. For more information about the database refer to the website [12].

FDMs for HLFSIM calculation were taken from VAIQ Database [8] created by Engelke.

Pearson linear correlation coefficient (PLCC) and Spearman rank order correlation coefficient (SROCC) were employed to calculate the correlation between subjective and objective quality evaluation results. No regression was performed. The calculation was done for every distortion type separately and for the whole database. The values of correlation coefficients could be found in Tab. 1. The best performer from FSIM and HLFSIM metrics is marked.

In cases where PLCC for HLFSIM (or $HLFSIM_C$) was higher than for FSIM ($FSIM_C$) the statistical significance of difference was calculated using Fisher r-to-z transformation. Resulting p-values are stated in Tab. 2. Considering significance level 0.05, p-values has to be lower than 0.05 to prove the significant difference between FSIM and HLFSIM performance. As can be seen, none of the modifications of HLFSIM is lower than the threshold which means that even though the correlation coefficient increased after addition of HLF information, the increase is not statistically significant. HLF information therefore does not improve the performance of the metric for types of distortions contained in the LIVE database.

4. Conclusion

This paper studies the influence of high level features (HLF) of human visual system on objective image quality assessment.

FSIM index [5] is one of the metrics which consider the different importance of the salient and non-salient areas in image for quality perception. However it was shown [17] that if the image is reconstructed according to regions of interest (ROI), low level features (LLF) extraction, used in FSIM, it is not sufficient for modeling visual attention and its quality evaluation does not agree with subjective tests.

Authors proposed modification of FSIM to calculate also with HLF by incorporating FDM into the metric. These are obtained from the eye-tracker which means that metric cannot be used in real-time applications. Also three LLF estimators were studied – Phase Congruency, Phase Spectrum of Fourier Transform and combination of both. The proposed metric is called HLFSIM.

It was shown, that for images reconstructed according to ROI, this information helps the metric to assess the quality of the images correctly for all three modifications.

Quantitative tests on LIVE database [12] should prove if it could improve the metric's performance even on the different types of distortions. PLCC and SROCC were used to calculate the correlation between subjective and objective assessment. The statistical significance of improvement was then calculated using Fisher r-to-z transform. The results show that the correlation coefficients increased in most cases but the improvement was not statistically significant. That means that the HLF information does not improve the metric performance for none of the modifications for images with distortion distributed all over the image space.

Acknowledgements

This work was partially supported by the COST IC1003 European Network on Quality of Experience in Multimedia Systems and Services – QUALINET, by the COST CZ LD12018 Modeling and verification of methods for Quality of Experience (QoE) assessment in multimedia systems – MOVERIQ and by the grant No. P102/10/1320 Research and modeling of advanced methods of image quality evaluation of the Czech Science Foundation.

Appendix

In Fig. 5 the computation scheme of $HLFSIM_{PC\&PFT}$ is shown. The inputs of the metric are reference image (f_1), distorted image (f_2) and FDM (HLF). All other parameters are the same as in FSIM. For $HLFSIM_{PC}$ ($HLFSIM_{PFT}$) LLF_1 and LLF_2 are already the outputs of PC (PFT) algorithm used on both images.

References

[1] *ITU-R Recommendation BT.500-13*. Methodology for the subjective assessment of the quality of television pictures. January 2012.

[2] SHEIKH, H. R., BOVIK, A. C. Image information and visual quality. *IEEE Transaction on Image Processing*, vol. 15, no. 2, February 2006, p. 430–444.

[3] WANG, Z., et al. Image quality assessment: From error visibility to structural similarity. *IEEE Transactions on Image Processing*, April 2004, vol. 13, no. 4, p. 600–612.

[4] WANG, Z., SIMONCELLI, E. P., BOVIK, A. C. Multi-scale structural similarity for image quality assessment. In *IEEE Asilomar Conference on Signal, Systems and Computers*, vol. 2, November 2003, p. 1398–1402.

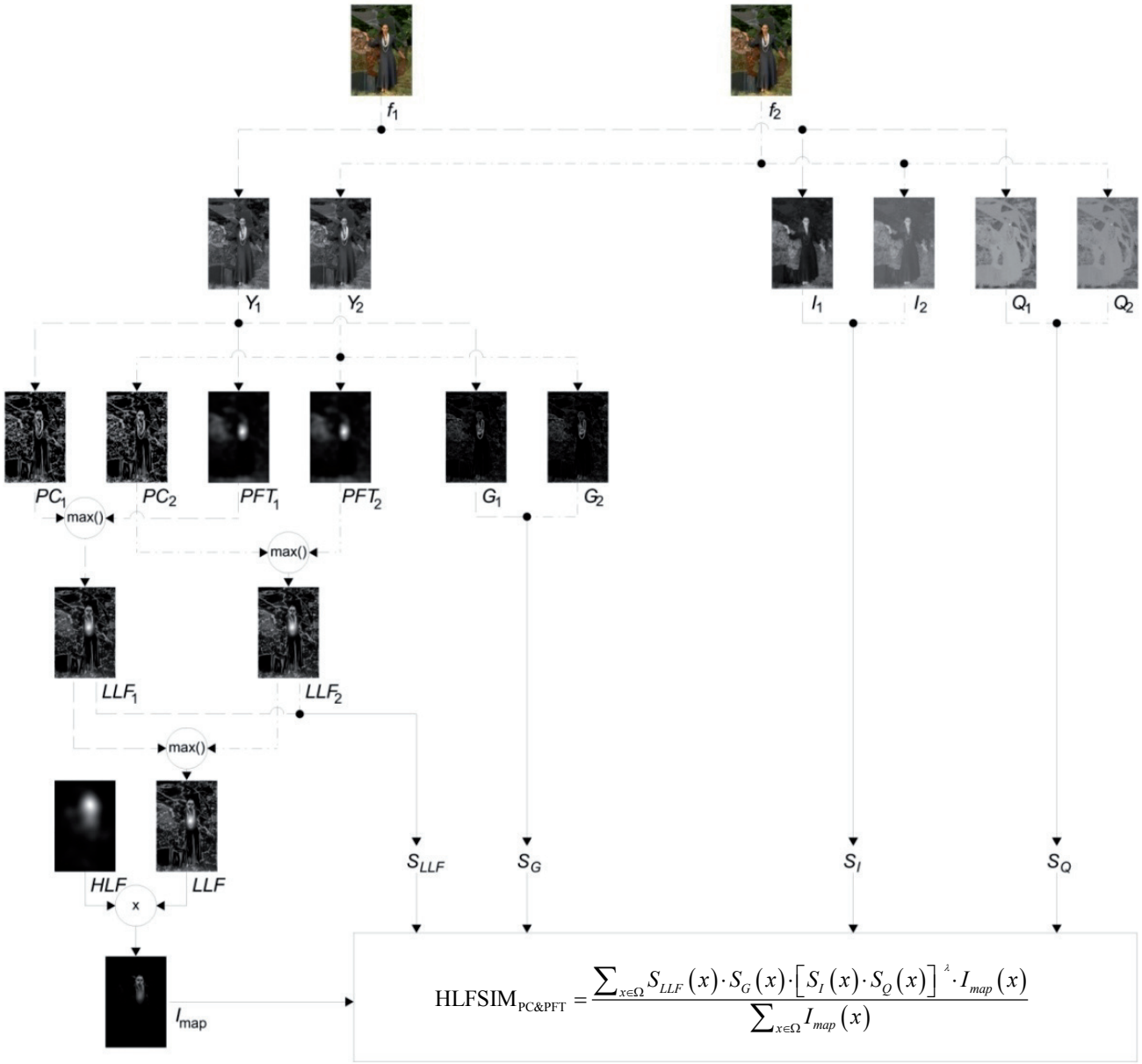

Fig. 5. The computation scheme of $\mathrm{HLFSIM}_{\mathrm{PC\&PFT}}$.

[5] ZHANG, L., et al. FSIM: A Feature Similarity Index for Image quality assessment. *IEEE Transactions on Image Processing*, August 2011, vol. 20, no. 8, p. 2378-2386.

[6] RAPANTZIKOS, K., AVRITHIS, Y., KOLIAS, S. Vision, attention control, and goals creation system. *Perception-Action Cycle. Springer Series in Cognitive and Neural Systems*, 2011, p. 363-386.

[7] THEEUWES, J. Top-down and bottom-up control of visual selection. *Acta Psychologica*, 2010, vol. 135, p. 77-79.

[8] ENGELKE, U., MAEDER, A., ZEPERNICK, H.-J. Visual attention modeling for subjective image quality databases. In *IEEE International Workshop on Multimedia Signal Processing*, October 2009, p. 1-6.

[9] DOSTAL, P., KRASULA, L., KLIMA, M. HLFSIM: Objective image quality metric based on ROI analysis. In *IEEE International Carnahan Conference on Security Technology (ICCST 2012)*, Oct. 2012, p. 367-375.

[10] MORRONE, M. C., ROSS, J., BURR, D. C., OWENS, R. Mach bands are phase-dependent. *Nature*, Nov. 1986, vol. 324, no. 6049, p. 250–253.

[11] KOVESI, P. D. Image features from Phase Congruency. *Videre: A Journal of Computer Vision Research*, MIT Press, 1999, vol. 1, no. 3.

[12] SHEIKH, H. R., et al. *LIVE Image Quality Assessment Database Release 2*, [Online]. http://live.ece.utexas.edu/research/quality.

[13] JÄHNE, B., HAUBECKER, H., GEIBLER, P. *Handbook of Computer Vision and Applications*. New York: Academic, 1999.

[14] YANG, C., KWOK, S. Efficient gamut clipping for color image processing using LHS and YIQ. *Opt. Eng.*, Mar. 2003, vol. 42, no. 3, p. 701–711.

[15] HOU, X., ZHANG, L. Saliency detection: A spectral residual approach. In *Conference on Computer Vision and Pattern Recognition*, 2007, p. 1-8.

[16] GUO, C., MA, Q., ZHANG, L. Spatio-temporal saliency detection using phase spectrum of quaternion Fourier transform. In *Conf. on Computer Vision and Pattern Recognition*, 2008, p. 1-8.

[17] DOSTAL, P., KLIMA, M. Locally adaptive demosaicing technique for security images based upon Region-of-Interest analysis. In *IEEE International Carnahan Conf. on Security Technology*. Piscataway, Oct. 2011, p. 1–10.

[18] HIRAKAWA, K., PARKS, T. W. Adaptive homogeneity-directed demosaicing algorithm. *IEEE Transaction on Image Processing*, 2005, vol. 14, no. 3, p. 360–369.

[19] MENON, D., ANDRIANI, S., CALVAGNO, G. Demosaicing with directional filtering and a posteriori decision. *IEEE Transaction on Image Processing*, 2007, vol. 16, no. 1, p. 132–141.

[20] ALLEYSON, D., SUSSTRUNK, S., HERAULT, J. Linear demosaicing inspired by HVS. *IEEE Transaction on Image Processing*, April 2005, vol. 14, no. 4, p. 439–449.

[21] CHUNG, K. L., et al. Demosaicing of Color Filter Array Captured Images Using Gradient Edge Detection Masks and Adaptive Heterogeneity-Projection. *IEEE Transaction on Image Processing*, Vol. 17, No. 12, December 2008, pp. 2356–2367.

[22] DE SIMONE, F., et al. Subjective evaluation of JPEG XR image compression. *Processing SPIE*, 2009, vol. 7443.

About Authors ...

Petr DOSTÁL graduated at the Czech Technical University (CTU) in Prague in 2008. Currently he is a Ph.D. student at the Faculty of Electrical Engineering, CTU. His research interests are oriented to image processing and image compression for security and multimedia applied imaging systems. He is actively involved in the COST Action IC1003 QUALINET.

Lukáš KRASULA was born in 1989. He graduated at the Czech Technical University in Prague in 2013. Currently he is a Ph.D. student at the Faculty of Electrical Engineering, Czech Technical University in Prague and at the University of Nantes. His research interests are oriented to image processing and image compression for security and multimedia applied imaging systems. He is actively involved in the COST Action IC1003 QUALINET.

Miloš KLÍMA was born in 1951. He is a Full Professor (from 2000) and the Head of the Department of Radio Electronics of the Faculty of Electrical Engineering of the Czech Technical University in Prague (from 2006). From 1989 he is a leader of the Multimedia Technology Group (MMTG) at the same department. His teaching field is the multimedia and television technology and photonics. His research activities are oriented to the image compression, image quality evaluation, HVS modeling and applied image photonics. He is the author or coauthor of over 150 publications.